Key Engineering Materials
ISSN: 1662-9795, Vol. 926, pp 1778-1785
doi:10.4028/p-4irh1n
© 2022 The Author(s). Published by Trans Tech Publications Ltd, Switzerland.
Submitted: 2021-12-21
Revised: 2022-01-28
Accepted: 2022-01-29
Online: 2022-07-22

Evaluation of the Rheological Behaviour of Magnetorheological Fluids Combining Bulge Tests and Inverse Analysis

Angela Cusanno[a*], Antonio Piccininni[b], Pasquale Guglielmi[c] and Gianfranco Palumbo[d]

Politecnico di Bari, Department of Mechanics, Mathematics and Management, Via Orabona 4 - 70125 Bari - Italy

[a]angela.cusanno@poliba.it, [b]antonio.piccininni@poliba.it, [c]pasquale.guglielmi@poliba.it, [c]gianfranco.palumbo@poliba.it

Keywords: Magnetorheological Fluids (MRF); hydraulic bulge tests; lightweight alloys; inverse analysis.

Abstract. Magnetorheological Fluids (MRFs) are included in the so called "smart materials": they are suspensions of magnetically responsive particles in a liquid carrier, whose rheological behaviour (e.g., its viscosity) can be changed quickly and reversibly if subjected to a magnetic field. Their application as forming medium in sheet metal forming processes is gaining interests in the recent years since the thickness and the strain distribution on the formed part can be affected by properly changing the properties of the MRF. In order to widely adopt MRFs in such processes, the evaluation of their rheological behaviour according to the applied magnetic field plays a key role. But there are still few works in the literature about the most effective way to characterise the MRFs to be used in sheet metal forming applications.

In this work, the rheological behaviour of a MRF is carried out by means of an inverse analysis approach using data from bulge tests performed using an MRF as forming medium. Bulge tests were conducted on sheets having known properties using an equipment with a solenoid to generate the magnetic field, which was specifically designed and manufactured. Pressure rate and magnetic flux density were varied according to a Design of Experiments (DoE) while the strain experienced by the sheet material was acquired by means of a Digital Image Correlation (DIC) system in order to compare it with the numerical one. In particular, the fitting between numerical and experimental data was obtained by changing the MRF's rheological properties using an inverse analysis technique. The proposed methodology allows to evaluate the MRF behaviour at different levels of both magnetic field and pressure rate, which are determinant for the FE simulation of sheet metal forming processes.

Introduction

With the aim of reducing energy consumption, nowadays the development of lightweight components - i.e. replacing conventional metallic materials with lighter alloys - is a great challenge in several sectors, such as automotive and aerospace fields [1, 2]. Thus, flexible forming technologies that allow to obtain complex shapes from lightweight alloys are needed. In the recent years, among other flexible forming processes (such as SuperPlastic Forming [3, 4], Incremental Forming [5, 6] and Hydroforming [7, 8]), Magnetorheological Pressure Forming (MRPF) is gaining interest since the thickness and the strain distribution on the formed part can be affected by properly changing the properties of the forming medium [9, 10]. In the case of MRPF, the forming medium is a magnetorheological Fluid (MRF). This kind of fluids are included in the so called "smart materials": they are based on a suspension of magnetically responsive particles in a liquid carrier, whose rheological behaviour (e.g., its viscosity) can be changed quickly and reversibly if subjected to a magnetic field [11]. Currently, MRFs are widely used in the automotive field for brakes [12] and clutches [13], in the biomedical field for prostheses [14] and for these applications there are already available constitutive models which are able to describe the field-dependent MRF characteristics (shear stress vs. shear rate) [15]. As for their applications within the manufacturing processes, they are used for finishing [16] and sheet metal forming operations [17, 18]. However, there are still few

This article is an open access article under the terms and conditions of the Creative Commons Attribution (CC BY) license (https://creativecommons.org/licenses/by/4.0)

studies in literature about the most effective way to characterise the MRFs when used for sheet metal forming applications: Wang et al. [19] used a combination of extrusion tests and FEM simulations to characterize a kind of MRF, in order to apply the obtained characterization to the simulation of bulge tests using MRF as forming medium.

In this work, the rheological behaviour of a MRF is carried out by means of an inverse analysis approach using data from bulge tests performed using an MRF as forming medium. Bulge tests were conducted on Aluminum Alloy sheets (AA5754-H111) having known properties. Numerical simulations were run reproducing the experimental loading conditions and varying the MRF's rheological properties (Young's Modulus, E [MPa] and Poisson's ratio, ν) according to an ordered full factorial plan. The error between numerical and experimental data was used as an output variable on which interpolant response surfaces were created. The metamodels were then used to carry out a virtual optimization aimed at calculating the optimal values of the input parameters (E and ν) able to minimize the error with the experimental data (basically according to an inverse analysis approach). The calibrated values were then validated on an additional loading condition, showing a good level of accordance.

Materials and Methodology

Materials. Experimental bulge tests were carried out using circular Aluminum Alloy (5754-H111) sheets 0.5 mm thick having a diameter of 66 mm, while a hydrocarbon oil-based MR fluid (MRHCCS4-A, supplied by Liquid Research Limited) with a packing fraction by weight of 70% was used as forming medium. In Fig. 1 the physical properties and the B-H curve of the MRF are shown, as well as the aluminum alloy flow curve. The latter was obtained by means of tensile tests, using an INSTRON 4485 universal testing machine controlled by a Zwick-Roell software, setting a crosshead speed of 6 mm/min. The experimental data were approximated by the Hollomon's equation [20], being the values of the strength coefficient, K and the strain-hardening exponent, n 326.2 MPa and 0.1743 respectively.

Property	Value
Operating Temperature	-40 [°C] to 140 [°C]
Density	2.49 [g/cc]
Colour	Grey
Flash Point	>190 [°C]

(a)

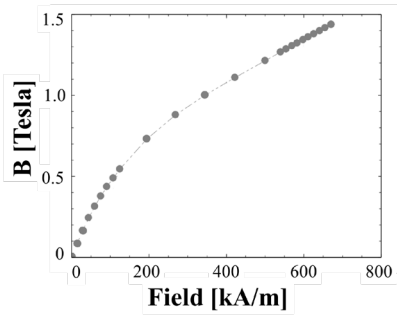

(b)

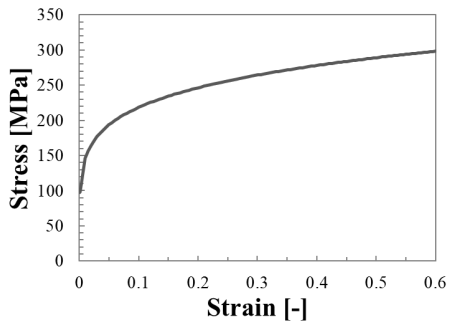

(c)

Fig. 1 (a) Physical properties and (b) B-H curve of the MRHCCS4-A; (c) AA5754-H111 Flow curve obtained from tensile tests.

Experimental bulge tests using MRF. The setup used for the experimental bulge tests is shown in Fig. 2. First, the cavity was filled with 100 ml of MRF, the blank was placed between the cavity and the die, then serrated to prevent any blank drawing. The inner diameter of the cavity and fillet radius of the die are 50 mm and 8 mm, respectively. The pressurized oil was introduced into the double-acting cylinder (connected to the punch), the MRF was squeezed, and, in turn, it transferred the loading pressure to the sheet. During the test, the oil pressure was controlled by a proportional valve connected to a hydraulic power unit and acquired by a pressure sensor, while the punch displacement was acquired by a linear digital scale. A solenoid combined with a DC power supply was used to generate a maximum magnetic flux density of 3.8 mT, using an input current of 2.6 A. After each test, the full-field distribution of strains was acquired by means of a Digital Image Correlation (DIC) system (ARAMIS, GOM), whereas the dome height was acquired by means of a

height gauge. A three-level full factorial design with two factors was considered as experimental plan. In particular, the oil pressure rate (0.5 – 2 –5 [bar/s]) and the applied magnetic flux density (0 – 1.8 – 3.8 [mT]) were considered as input parameters. Once the pressure reached 250 bar, it was held for 40 seconds and then the test was stopped. Among the tests, the ones characterized by a pressure rate of 0.5 [bar/s] and 5 [bar/s] were used for the inverse analysis procedure, whereas the loading conditions characterized by a pressure rate of 2 [bar/s] were used to validate the results of the inverse analysis.

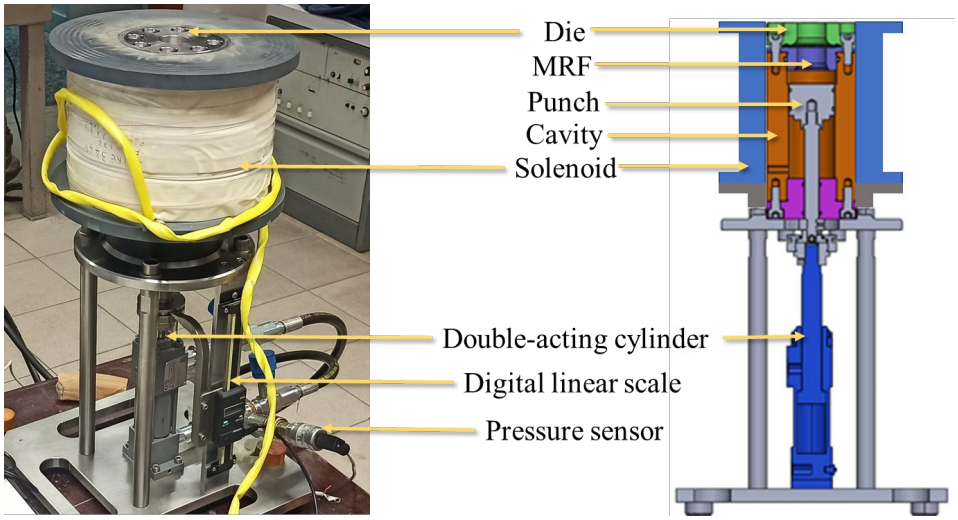

Fig. 2 Equipment for the bulge tests using MRF as forming medium.

FE model for bulge tests. Bulge tests were simulated using the commercial software ABAQUS/Explicit. To reduce the computational cost, an axisymmetric FE model was used; it is shown in Fig. 3. The sheet and the MR Fluid were modelled as deformable bodies: the former was meshed with 250 elements, whereas the latter with 2550 and progressively reducing the average size of the element in the proximity of the contact with the blank. Moreover, in order to avoid excessive distortions of the MRF elements, an adaptive mesh with a frequency of 10 increments with 5 remeshing sweeps per increment was set. No damage criterion was implemented to determine material failure. At first, the loading conditions regarding the two pressure rates of 0.5 and 5 [bar/s] were simulated.

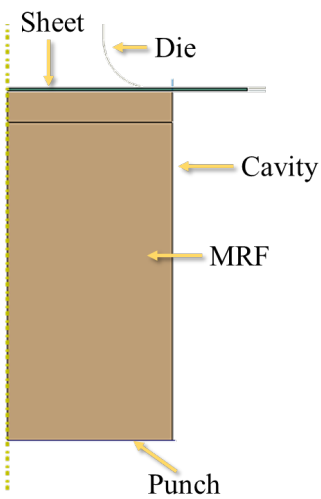

Fig. 3 Scheme of the FE model.

Simulations were performed assigning to the punch both the speed and the test duration resulting from the experimental tests. Values of the Young Modulus, E [MPa] and Poisson's ratio, ν were varied according to a full factorial DoE with 3 levels (1- 5 -15 [MPa] and 0.35 – 0.4 – 0.49 for E and ν respectively). The final values of dome height and major strain were collected as numerical outputs to be compared with the experimental ones.

Inverse analysis methodology. The inverse analysis approach was treated as an optimization problem, being the final aim the minimization of an error function that quantifies the discrepancy between the numerical data and the experimental ones. The proposed methodology, schematically depicted in Fig. 4, was applied to calibrate the rheological parameters in each of the investigated levels of the magnetic flux density (as described in the previous section).

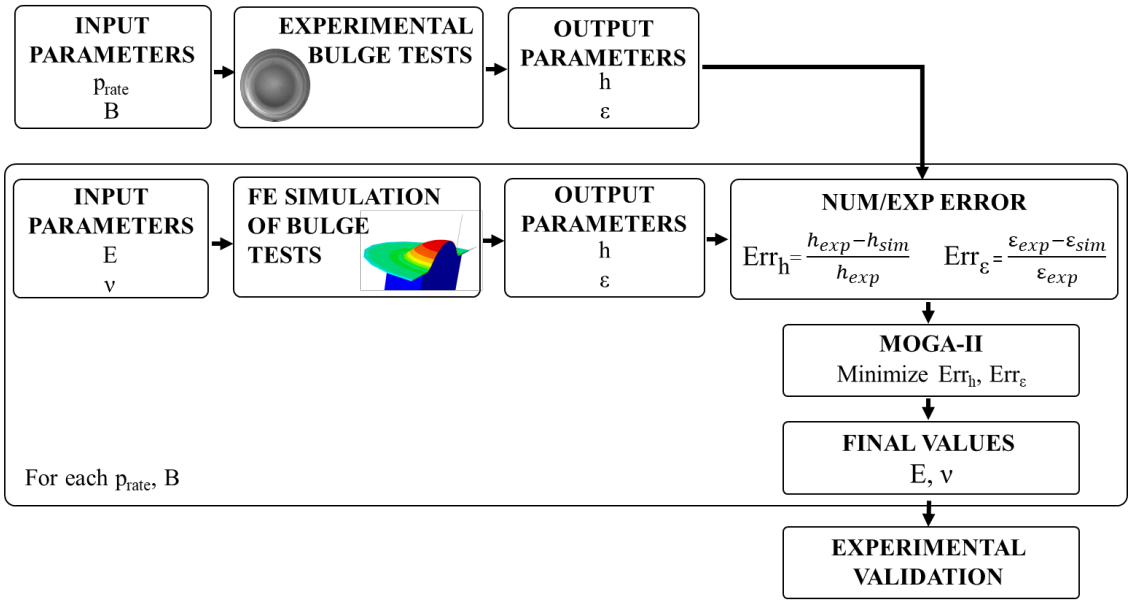

Fig. 4 Methodology for the inverse analysis.

Results from numerical simulations were collected in terms of final h and ε that were, in turn, used to calculate the error with the experimental data (strains from ARAMIS and dome height from the gauge) according to Eq. 1 and Eq. 2.

$$Err_h = \frac{h_{exp}-h_{sim}}{h_{exp}} \quad (1)$$

$$Err_\varepsilon = \frac{\varepsilon_{exp}-\varepsilon_{sim}}{\varepsilon_{exp}} \quad (2)$$

Response Surfaces (RS) were created on the two error parameters by choosing the most accurate interpolating algorithm among the five Radial Basis Functions available within the integration platform modeFRONTIER. The constructed RS were then used as starting point for a virtual optimization: each error variable was then linked to a minimizing objective function. The optimization round, managed by a multi-objective genetic algorithm (MOGA-II), was based on 1000 successive generations, each composed of 9 individuals (as the initial DoE). At the end of the optimization round, optimal designs could be eventually evaluated: those designs were characterized by the optimal values of the defined input parameters (E and ν) able to minimize the error with the experimental data. The optimization round was repeated for all the investigated magnetic flux densities and pressure rates. After the optimization procedure, an additional set of simulation for the intermediate value of pressure rate (2 [bar/s]) was performed with the optimal values of E and ν resulting from the inverse analysis approach, in order to validate the methodology.

Results and Discussion

Experimental bulge tests results. In Fig. 5**,** the main results coming from the experimental bulge tests using MRF as forming medium are summarized. It can be noticed that, for all the magnetic flux density conditions, higher values of dome height and major strain could be reached when increasing the pressure rate (Fig. 5a, b).

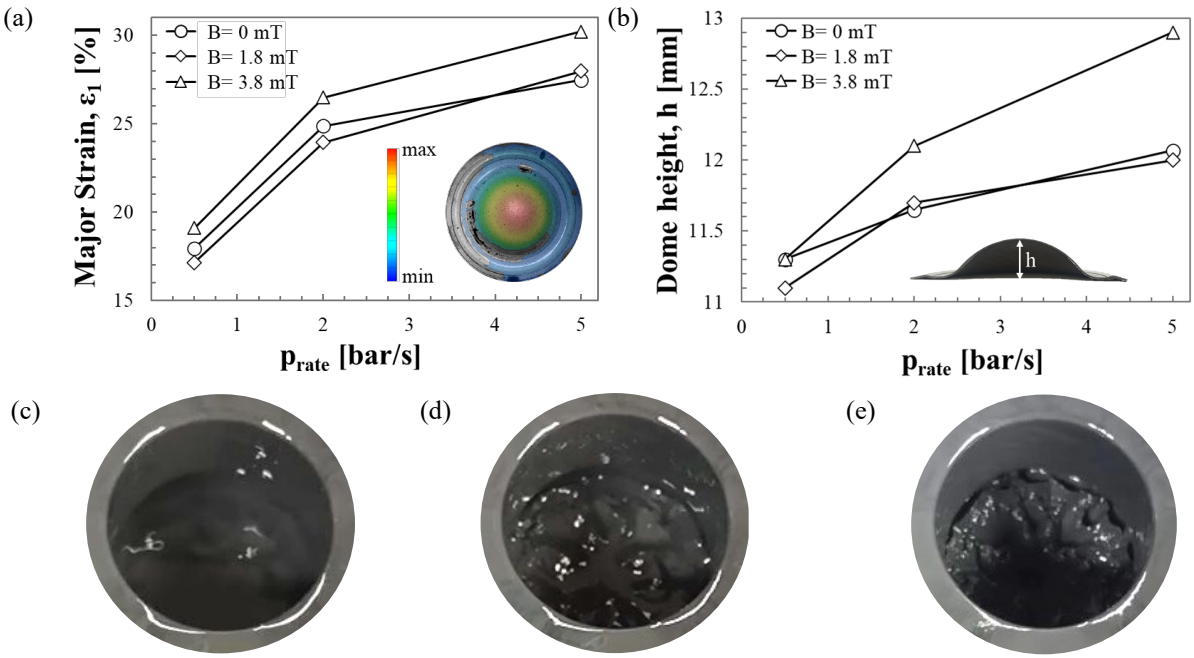

Fig. 5 (a) Major Strain at the dome and (b) Dome height reached during bulge tests according to the imposed pressure rate and applied magnetic field; (c) MR Fluid MRHCCS4-A without magnetic field; (d) MR Fluid MRHCCS4-A when a Magnetic flux density, B= 1.8 mT is applied; (d) MR Fluid MRHCCS4-A when a Magnetic flux density, B= 3.8 mT is applied.

On the other hand, concerning the different applied magnetic field values, when applying 3.8 mT, an improvement in major strain and dome height values could be noticed; on the other hand, a less evident difference could be noticed if the flux density was increased from 0 mT to 1.8 mT. These results suggest that changes in the MR Fluid rheological behaviour occurred when a magnetic field higher than 1.8 mT was applied. This was confirmed by the macroscopic analysis of the MR Fluid according to the magnetic field (Fig. 5c, d, e): only in the case of 3.18 mT a significant change in the texture can be noticed.

Results of FE simulation plan of bulge tests. Table 1 shows a summary of the values of the dome height (h) and major strain at the dome (ε), resulting from the simulation plan, in the case of a pressure rate of 0.5 bar/s and 5 bar/s. It is worth mentioning that there were specific combinations of the input parameters that led to higher value of the monitored output variables. Nevertheless, all the data were listed in the table. It can be also noticed that the selected range of E and ν allowed to obtain values of h from 0.73 to 38.21 mm and values of ε in the range 0.025 – 280 %, thus including also obtained experimental values (summarized in Fig. 5).

Table 1 Dome height, h [mm] and Major Strain at the dome, ε [%] resulting from the simulation plan.

		p_{rate}=0.5 bar/s		p_{rate} =5 bar/s	
E [MPa]	**ν**	**h [mm]**	**ε [%]**	**h [mm]**	**ε [%]**
1	0.35	0.73	0.01	0.76	0.025
1	0.4	0.89	0.05	0.92	0.056
1	0.49	3.3	1.3	3.44	1.5
5	0.35	1.73	0.3	1.8	0.34
5	0.4	2.19	0.5	2.28	0.58
5	0.49	8.97	13.97	9.7	16.72
15	0.35	3.3	1.31	3.44	1.56
15	0.4	4.2	2.48	4.41	2.68
15	0.49	36.29	268	38.21	280

Investigation about the prediction of E and ν resulting from the inverse analysis. The adopted inverse analysis procedure, which combined the results from a subset of the experimental data with the numerical results of the simulation plan, allowed to obtain the optimal values of E and ν for two investigated conditions in terms of magnetic flux density (0 mT and 3.8 mT). It can be noticed that, as summarized in Fig. 6b, values of E varied from 5.81 MPa (in absence of magnetic field and for the lowest pressure rate) to 7 MPa (for the highest values of both magnetic field pressure rate). In addition, the results from the optimization suggested that the Poisson's ratio could be considered as a constant value regardless of the applied magnetic field and pressure rate values. Moreover, from Fig. 6a it can be also noticed that Young's Modulus is mainly influenced by the applied magnetic field density (in accordance with the work by Liu et al.[21]), whereas it slightly increases according to the pressure rate.

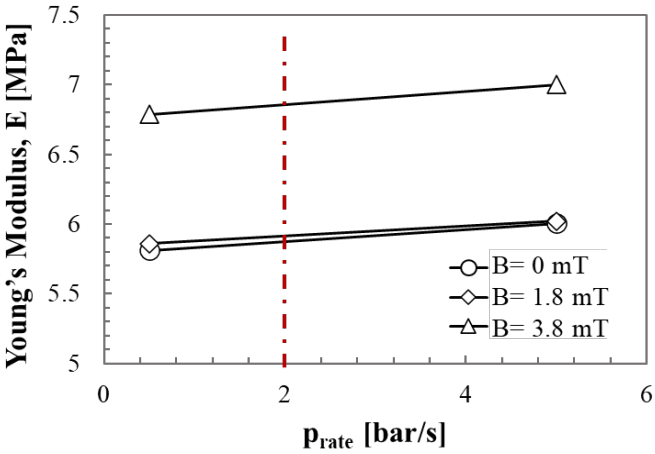

(a)

B [mT]	p_{rate} [bar/s]	E [MPa]	ν
0	0.5	5.81	0.49
0	5	6.00	0.49
1.8	0.5	5.86	0.49
1.8	5	6.02	0.49
3.8	0.5	6.79	0.49
3.8	5	7.00	0.49
0	2	5.87	0.49
1.8	2	5.91	0.49
3.8	2	6.86	0.49

(b)

Fig. 6 (a) Trend of Young's Modulus, *E* [MPa] according to pressure rate, p_{rate} [bar/s] resulting from the inverse analysis procedure; (b) summary of values of E and ν after the the inverse analysis procedure for p_{rate}= 0.5 [bar/s] and p_{rate}= 5 [bar/s]; E and ν prediction for p_{rate}= 2 [bar/s].

In order to validate the methodology, the experimental loading conditions at pressure rate equal to 2 [bar/s] were simulated: a constant value of ν=0.49 was used for the validation, whereas the values of the Young's Modulus were linearly extrapolated as shown in Fig. 6a. Fig. 7 reports a general overview of the results, combining those coming from the inverse analysis (at the magnetic flux densities of 0 mT and 3.8 mT) with those coming from the numerical simulations run for validation purposes.

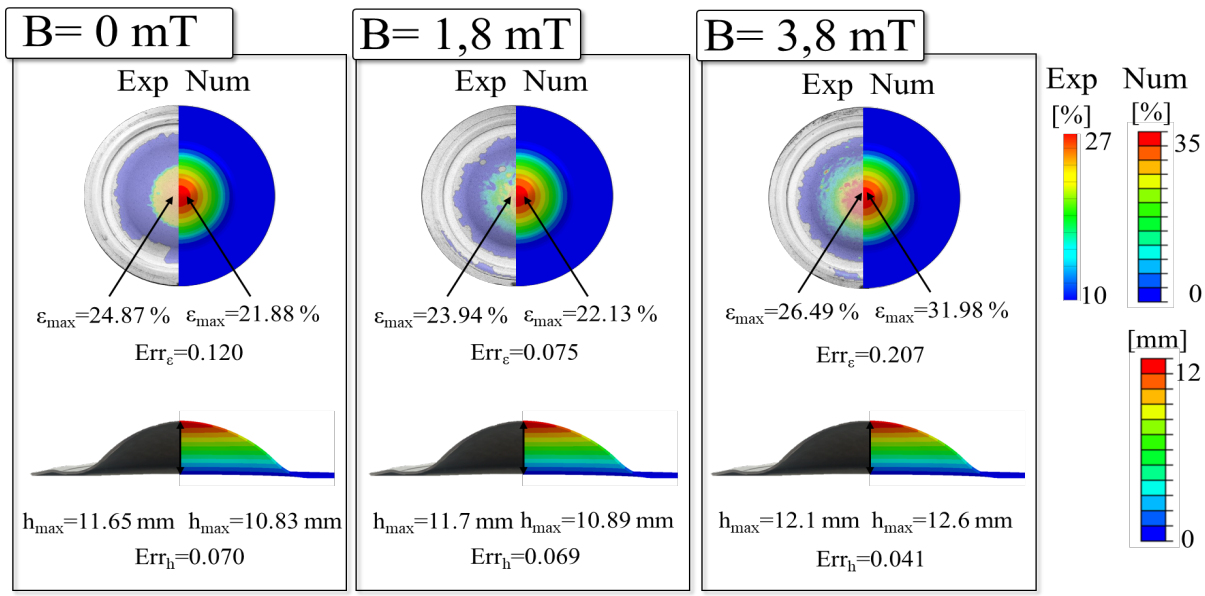

Fig. 7 Experimental vs. numerical results of the validation of the procedure (p_{rate}=2 bar/s).

The discrepancy reported in Fig. 7 were equal to 0.07 (0 mT), 0.069 (1.8 mT) and 0.041 (3.8 mT) regarding the final dome height; as for the final major strain, the errors were equal to 0.12 (0 mT), 0.076 (1.8 mT) and 0.21 (3.8 mT).

Conclusions

In the present work, the rheological behaviour of a MRF was analysed by means of an inverse analysis approach using data from bulge tests performed using the investigated MRF as forming medium. Experimental results showed that both increasing pressure rates and magnetic field values, higher dome heights and strain levels can be reached, thus suggesting a change in the MRF rheological behaviour.

The inverse analysis approach, based on the construction of accurate RS, showed good potentialities since it provided optimal values of the defined input parameters that resulted to be effectively descriptive of the MRF behaviour. Moreover, the definition of a virtual optimization made possible the investigation of several potential optimal designs requiring very limited computational costs. Results from the adopted inverse analysis procedure showed that the rheological behaviour of the MRF is affected by the applied pressure rate and the surrounding magnetic field mainly in terms of the Young's Modulus value, whereas the Poisson's ratio could be considered as a constant value regardless of the operative conditions. Future works will be focused not only on the investigation of more levels of both magnetic field and pressure rates, but also on more refined constitutive equations to further improve the prediction capabilities of the proposed methodology.

References

[1] D. Kumar, R. K. Phanden, L. Thakur, A review on environment friendly and lightweight Magnesium-Based metal matrix composites and alloys, Mater. Today Proc. 38 (2021) 359–364

[2] C. Han, Research on the Development and Application of Lightweight Automotive Materials, J. Phys. Conf. Ser. 1676 (2020) 012085

[3] D. Sorgente, A. Lombardi, D. Coviello, L. D. Scintilla, M. Fontana, A strain-dependent model for the coefficient of friction in the tool-blank interaction in superplastic forming, J. Manuf. Process. 73 (2022) 791–798

[4] P. Guglielmi, A. Cusanno, I. Bagudanch, G. Centeno, I. Ferrer, M.L. Garcia-Romeu, G. Palumbo, Experimental and numerical analysis of innovative processes for producing a resorbable cheekbone prosthesis, J. Manuf. Process. 70 (2021) 1–14

[5] S. Pandre, A. Morchhale, N. Kotkunde, S. Kurra, Processing of DP590 steel using single point incremental forming for automotive applications 36 (2021) 1658–1666

[6] G. Palumbo, A. Piccininni, G. Ambrogio, E. Sgambitterra, Design of custom cranial prostheses combining manufacturing and drop test finite element simulations, Int. J. Adv. Manuf. Technol. 111 (2020) 1627–1641

[7] Y. M. Hwang, K. I. Manabe, Latest Hydroforming Technology of Metallic Tubes and Sheets, Met. 11 (2021) 1360

[8] G. Palumbo, Hydroforming a small scale aluminum automotive component using a layered die, Mater. Des. 44 (2013) 365–373

[9] P. yi Wang, W. zhuo Zhang, Z. jin Wang, J. Yi, Effect of viscosity of viscous medium on formability of Al1060-O sheet in viscous pressure forming (VPF): an experimental study, Int. J. Adv. Manuf. Technol. 87 (2016) 677-686

[10] Y. Y. Mu, F. Li, C. Li, Y. Q. Zang, J. Xu, Mechanism of pre-deformation effect on sheet deep-drawing forming under magnetic field condition using a magnetorheological fluid (MRF) medium, Int. J. Adv. Manuf. Technol. 116 (2021) 863–875

[11] X. Zhu, X. Jing, L. Cheng, Magnetorheological fluid dampers: A review on structure design and analysis, J. Intell. Mater. Syst. Struct. 23 (2012) 839–873

[12] B. K. Kumbhar, S. R. Patil, S. M. Sawant, Synthesis and characterization of magneto-rheological (MR) fluids for MR brake application, Eng. Sci. Technol. an Int. J. 18 (2015) 432–438

[13] F. Bucchi, P. Forte, F. Frendo, Experimental characterization of a permanent magnet magnetorheological clutch for automotive applications, ASME 2012 11th Bienn. Conf. Eng. Syst. Des. Anal. ESDA 2012, 4 (2012) 345–355

[14] O. Arteaga, A. Cevallos, M. I. Erazo, K. D. Morales, D. B. Tenezaca, E. M. Argüello, Application of magnetorheological fluids in the design of a leg prosthesis with active damping, MATEC Web Conf. 192 (2018) 1–4

[15] M. Ashtiani, S. H. Hashemabadi, A. Ghaffari, A review on the magnetorheological fluid preparation and stabilization, J. Magn. Magn. Mater. 374 (2015) 711–715

[16] L. N. Pattanaik, H. Agarwal, Development of Magnetorheological Finishing (MRF) Process for Freeform Surfaces, Int. J. Adv. Mech. Eng. 4 (2014) 611–618

[17] F. Li, F. J. Zhou, M. N. Wang, S. Y. Zhu, C. C. Jin, New processing research on sheet metal bidirectional pressure forming using a magnetorheological fluid, Int. J. Adv. Manuf. Technol. 88 (2017) 923–929

[18] P. yi Wang, Z. jin Wang, N. Xiang, S. peng Cai, Z. xin Li, Mechanism of magnetic field condition on deformation behavior of sheet metal using a property-adjustable flexible-die, Int. J. Adv. Manuf. Technol. 109 (2020) 629-644

[19] P. Wang, Z. Wang, Journal of Magnetism and Magnetic Materials Determination of the flow stress of a magnetorheological fluid under three-dimensional stress states by using a combination of extrusion test and FEM simulation, J. Magn. Magn. Mater. 419 (2016) 255–266

[20] H. Hollomon, Tensile deformation., Aime Trans 12 (1945) 1–22

[21] H. Liu, Q. Luo, J. Wu, T. Li, Y. Q. Wang, Performance analysis of MRF-based flexible supporting of thin-walled part, ICMRE Int. Conf. Proceedings (2018) 132–136